Electrostatic Properties of Membranes Containing Acidic Lipids and Adsorbed Basic Peptides: Theory and Experiment

Diana Murray,*,§ Anna Arbuzova,* Gyöngyi Hangyás-Mihályné,* Alok Gambhir,* Nir Ben-Tal,# Barry Honig,§ and Stuart McLaughlin*

*Department of Physiology and Biophysics, Health Sciences Center, SUNY Stony Brook, Stony Brook, New York 11794-8661 USA; #Department of Biochemistry, Tel-Aviv University, Ramat-Aviv, Tel-Aviv 69978, Israel; and §Department of Biochemistry and Molecular Biophysics, Columbia University, New York, New York 10032 USA

ABSTRACT The interaction of heptalysine with vesicles formed from mixtures of the acidic lipid phosphatidylserine (PS) and the zwitterionic lipid phosphatidylcholine (PC) was examined experimentally and theoretically. Three types of experiments showed that smeared charge theories (e.g., Gouy-Chapman-Stern) underestimate the membrane association when the peptide concentration is high. First, the zeta potential of PC/PS vesicles in 100 mM KCl solution increased more rapidly with heptalysine concentration (14.5 mV per decade) than predicted by a smeared charge theory (6.0 mV per decade). Second, changing the net surface charge density of vesicles by the same amount in two distinct ways produced dramatically different effects: the molar partition coefficient decreased 1000-fold when the mole percentage of PS was decreased from 17% to 4%, but decreased only 10-fold when the peptide concentration was increased to 1 μM. Third, high concentrations of basic peptides reversed the charge on PS and PC/PS vesicles. Calculations based on finite difference solutions to the Poisson-Boltzmann equation applied to atomic models of heptalysine and PC/PS membranes provide a molecular explanation for the observations: a peptide adsorbing to the membrane in the presence of other surface-adsorbed peptides senses a local potential more negative than the average potential. The biological implications of these "discreteness-of-charge" effects are discussed.

INTRODUCTION

The plasma membrane association of several peripheral membrane proteins, e.g., Src, K-Ras, MARCKS, and HIV-1 Gag, requires the electrostatic interaction of a cluster of basic residues on the protein with acidic lipids in the membrane (McLaughlin and Aderem, 1995; Resh, 1996; Bhatnagar and Gordon, 1997; Murray et al., 1997; Garnier et al., 1998). Adsorption to the plasma membrane is crucial for the activity and regulation of these proteins. For example, removing the N-terminal basic residues of Src weakens its partitioning onto phospholipid vesicles containing acidic lipids and produces nontransforming phenotypes in biological cells (Kaplan et al., 1990; Sigal et al., 1994; Resh, 1996). There is mounting evidence that similar, nonspecific electrostatic interactions may be important for the function and plasma membrane association of other proteins, including AKAP79 (Dell'Acqua et al., 1998), phosphatidylinositol phosphate kinase (Roa et al., 1998), G-protein coupled receptor kinases (Pitcher et al., 1998), and Numb (Knoblich et al., 1997). Many of these proteins are known to exist at high concentrations in localized regions of the plasma membrane. For example, MARCKS is concentrated at nascent phagosomes in macrophages (Allen and Aderem, 1996), AKAP79 is enriched in the postsynaptic region of neuronal cells (Dell'Acqua et al., 1998), and HIV-1 Gag self-assembles into lateral domains on the cytoplasmic surface of the plasma membrane of infected cells before viral budding (Garnier et al., 1998). We are interested in understanding the electrostatic properties of membranes that contain high surface concentrations of proteins with clusters of basic residues.

Experimental studies have characterized the membrane association of peptides corresponding to basic sequences in some of the proteins listed above (Kim et al., 1994; Buser et al., 1994; Zhou et al., 1994; Ghomashchi et al., 1995; Ben-Tal et al., 1996; Leventis and Silvius, 1998). Nonspecific electrostatic interactions between the basic residues and acidic lipids provide the main driving force for association with lipid bilayers; the binding depends only weakly on the chemical nature of either the basic residues or monovalent acidic lipid (Ben-Tal et al., 1996). Recent theoretical work based on finite-difference solutions to the nonlinear Poisson-Boltzmann equation (FDPB method) for atomic models of peptides and membranes describes well the electrostatic component of the membrane association of basic peptides (Ben-Tal et al., 1996, 1997; Murray et al., 1997, 1998). Specifically, the methodology correctly predicts how the membrane partitioning increases as the number of basic residues in the peptide increases, as the mole percentage acidic lipid in the membrane increases, and as the ionic strength of the solution decreases. So far, this approach has been applied only to the case where the peptide concentration is sufficiently low that interactions between membrane-adsorbed peptides can be ignored. Here we extend the calculations to conditions of higher peptide concentration to

Received for publication 20 May 1999 and in final form 2 September 1999.

Address reprint requests to Dr. Stuart G. McLaughlin, Department of Physiology and Biophysics, Health Sciences Center, SUNY Stony Brook, Stony Brook, NY 11794-8661. Tel.: 516-444-3615; Fax: 516-444-3432; E-mail: smcl@epo.som.sunysb.edu.

0006-3495/99/12/3176/13 $2.00

examine the effect of electrostatic interactions between membrane-adsorbed peptides. Fig. 1 outlines our theoretical approach to the problem based on FDPB calculations of atomic models of peptide/membrane systems.

Fig. 1 *A* illustrates that electrostatic equipotential profiles above a membrane containing 33 mol% acidic lipid in 100 mM monovalent salt solution are flat; e.g., the −25-mV equipotential profile (*red line*) is located ~10 Å above the membrane surface, in agreement with the prediction from Gouy-Chapman theory; this treatment models the acidic lipids in the membrane as a uniform surface charge density (Peitzsch et al., 1995). These predictions agree with experimental measurements from many different laboratories, which have established that the electrostatic properties of membranes containing monovalent acidic lipids can be described adequately by smeared charge theory when the aqueous solution contains only small monovalent or divalent ions (McLaughlin et al., 1981; Winiski et al., 1986; Hartsel and Cafiso, 1986; McLaughlin, 1989).

Fig. 1 *B* illustrates the interaction of a single heptalysine (specifically, acetyl-heptalysine-amide; valence $Z = +7$) with the membrane depicted in Fig. 1 *A*. The positive potential due to the peptide perturbs the negative potential of the membrane only in the vicinity of the peptide, as expected intuitively. As more peptide binds to the membrane, we anticipate that the average potential, or the zeta potential, of PC/PS vesicles will increase more steeply with the peptide concentration than predicted by smeared charge theories. (The zeta potential is the average electrostatic potential at the hydrodynamic plane of shear, which is ~0.2 nm from the surface of PC/PS vesicles in 100 mM monovalent salt (McLaughlin, 1989).) In electrochemistry literature, this is termed an "Esin-Markov" effect, which has long been attributed to the discrete nature of the charge on the

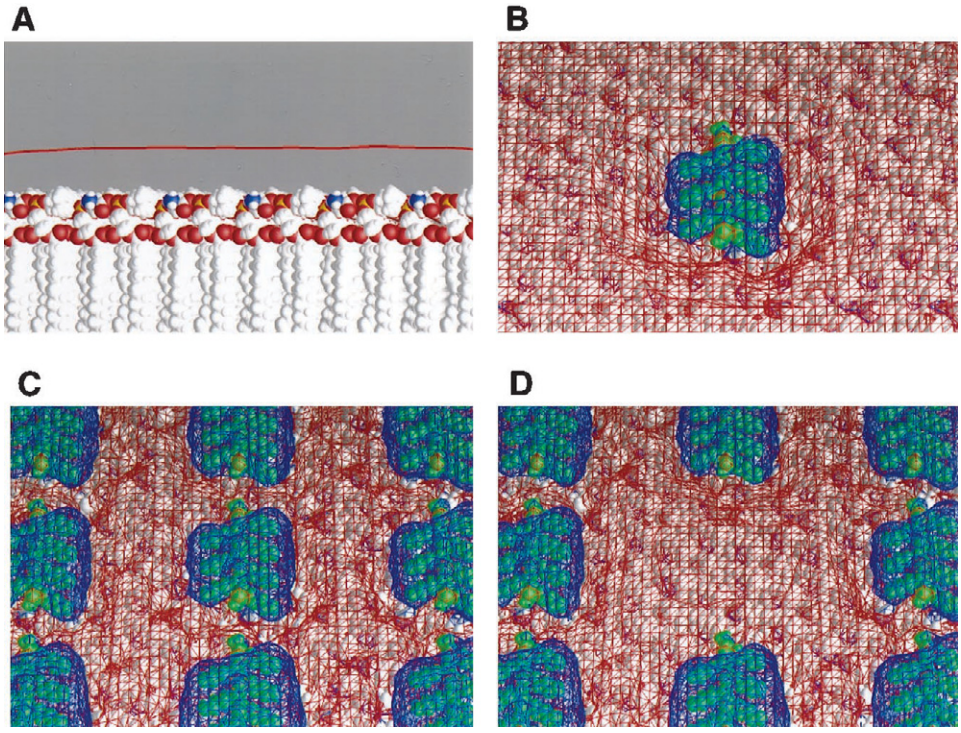

FIGURE 1 FDPB calculations of the electrostatic interaction of heptalysine with a 2:1 PC/PS membrane in 100 mM KCl. In the molecular models, each lipid occupies ~70 Å^2 within the plane of the membrane, the center-to-center distance between two nearest neighbor acidic lipids is ~15 Å, the dimensions of a single peptide are 17 Å × 31 Å × 7 Å, and the center-to-center distance between two adjacent peptides in the array of panel *C* is 42 Å in the horizontal direction and 37 Å in the vertical direction; the Debye length is ~10 Å. (*A*) The electrostatic equipotential contours above a 2:1 PC/PS membrane in the absence of heptalysine are flat. The red curve represents the −25-mV equipotential. In all panels, the potentials illustrated were calculated by solving numerically the nonlinear Poisson-Boltzmann equation for atomic models of heptalysine/membrane systems. In the membrane, oxygen atoms are colored red, nitrogen is blue, phosphorous is yellow, and carbon and hydrogen are white. (*B*) The adsorption of a single heptalysine to the membrane from panel *A* perturbs the electrostatic potential of the membrane in a localized region. In panels *B*, *C*, and *D*, the membrane is viewed from above, the red and blue meshes represent, respectively, the −25 and +25 mV equipotential profiles, the peptides are green, and the membrane is white; we assume the peptides do not change the location of the acidic lipids. (*C*) The adsorption of sufficient heptalysine to neutralize the membrane in panel *A* (net charge of the peptide array equals the net charge of the acidic lipids; one heptalysine per seven acidic lipids) produces a highly nonuniform electrostatic potential. Although the average charge density is zero, there are regions of significant negative and positive local potential. In the figure, the peptides are arranged uniformly at the membrane surface; departures from uniformity are considered in the text. (*D*) A heptalysine associating with the membrane when the surface concentration of peptide is high experiences a local potential that is significantly more negative than the average potential. The peptide at the center of the array in panel *C* has been removed to reveal the strong negative potential with which the peptide interacts. The electrostatic free energy of interaction of a peptide with the membrane in the presence of the array pictured here is only 1 kcal/mol weaker than the electrostatic free energy of interaction of a peptide with the membrane in the absence of other peptides (the interaction depicted in panel *B*; see Table 2).

adsorbing multivalent ion (Grahame, 1958; Levine et al., 1967; Barlow and MacDonald, 1967).

Fig. 1 *C* depicts the electrostatic interaction of heptalysine with the membrane of Fig. 1 *A* when the surface concentration of peptide is high enough to neutralize the negative surface charge density of the membrane: each heptalysine associates, on average, with seven acidic lipids. Although the average potential is zero, the FDPB calculations indicate there should be regions of negative and positive local potential. This suggests that a peptide adsorbing to a membrane under these conditions experiences a potential significantly more negative than that predicted by smeared charge theory (which is zero, because the surface charge density is zero). This is illustrated by Fig. 1 *D*, where the potentials were calculated with the central peptide removed. The −25 mV potential contour at the center of the membrane extends almost as far into the aqueous solution as it does in the absence of peptide (Fig. 1 *A*), demonstrating that attractive electrostatic interactions between the central peptide and the membrane can be obtained even when the net charge of the peptide/membrane system is zero.

The FDPB electrostatic method has been applied successfully to atomic models of proteins and nucleic acids for over 10 years (Honig and Nicholls, 1995). These studies have established that smeared charge models cannot describe effects such as charge-charge interactions or complex patterns of electrostatic potential that depend upon the specific location of charged and polar groups as well as a molecule's geometric shape. In this report, we apply the atomic-level FDPB approach to the membrane binding of basic peptides. Specifically, we measured experimentally the effect of high concentrations of unlabeled heptalysine on both the zeta potential of PC/PS vesicles and the membrane association of fluorescently labeled heptalysine, then used atomic models of membranes with multiple adsorbed polyvalent peptides to describe theoretically the electrostatic properties of these systems.

MATERIALS AND METHODS

Materials

1-Palmitoyl-2-oleoyl-sn-glycero-3-phosphatidylcholine (PC), 1-palmitoyl-2-oleoyl-sn-glycero-3-phosphatidylserine (PS), 1-palmitoyl-2-oleoyl-sn-glycero-3-phosphatidylglycerol (PG), 1-oleoyl-2-[12[(7-nitro-2,1,3-benzoxadiazol-4-yl)amino]dodecanoyl]-[phosphatidylcholine] (NBD-PC), and 1-oleoyl-2-[12[(7-nitro-2,1,3-benzoxadiazol-4-yl)amino] dodecanoyl]-[phospho-L-serine] (NBD-PS) were purchased from Avanti Polar Lipids (Alabaster, AL). Radiolabeled 1,2-di[1-^{14}C]oleoyl-L-3-phosphatidylcholine ([^{14}C]PC) was purchased from Amersham (Arlington Heights, IL), and 6-acryloyl-2-dimethylaminonaphthalene (acrylodan) was from Molecular Probes (Eugene, OR). The standard buffer solution contained 100 mM KCl buffered to pH 7 with 1 mM 3-(*N*-morpholino)propanesulfonic acid (MOPS).

Methods

Peptide synthesis and labeling

Heptalysine with blocked N (acetyl) and C (amide) terminals (net charge +7) was from either Chiron Technologies (Clayton Victoria, Australia; >50% pure) or the American Peptide Company (Sunnyvale, CA; >80% pure); identical results were obtained with the two peptide samples. The CKKKKKKK-amide (net charge +8) peptide was synthesized at the Center for Analysis and Synthesis of Macromolecules, SUNY, Stony Brook, and labeled on the cysteine with acrylodan by a procedure described by McIlroy et al. (1991). The acetyl-KKKKKKKC-amide (net charge +7) peptide was from Chiron Technologies and was labeled with acrylodan. After labeling, peptides were purified by a reverse-phase C8 high-performance liquid chromatography column. The purified peptides were examined using mass spectrometry and yielded *m*/*z* values of 1242 (+8) and 1287 (+7), consistent with the expected molecular weight for the labeled peptides. Acrylodan-labeled F159C-MARCKS(151–175), acetyl-KKKKKRFSCKKSFKLSGFSFKKNKK-amide, was a generous gift from D. Cafiso. Peptides were dissolved in 2× distilled water and stored in aliquots at −20°C. The relatively inexpensive peptide used for the charge reversal experiments, poly-L-lysine with MW of ~1000, was obtained from Sigma (St. Louis, MO).

Vesicle preparation

The initial concentration of lipids in chloroform was measured on a Cahn electrobalance, a method that gives the same results as phosphate analysis (Kim et al., 1991). Trace amounts of [^{14}C]PC were added to the lipid mixture to determine the final lipid concentration. Lipid mixtures were dried on a rotary evaporator and resuspended in the standard buffer to obtain multilamellar vesicles. Large unilamellar vesicles (LUVs) were made by extruding multilamellar vesicles 10 times through a stack of two polycarbonate filters (100-nm pore diameter) after five freeze-thaw cycles (Hope et al., 1985). All preparations and measurements were done at room temperature, 22–23°C, except for the electrophoretic mobility measurements, which were performed at 25°C.

Electrophoretic mobility measurements

The electrophoretic mobility, u, of multilamellar vesicles (Bangham et al., 1974) was measured in a Rank Brothers Mark I instrument (Bottisham, Cambridge, UK) as described previously (Cafiso et al., 1989). In these experiments, [lipid] ≪ [peptide]; in other words, the free peptide concentration is approximately equal to the total peptide concentration because the vesicles bind a negligible fraction of the peptide.

Equilibrium binding measurements

We studied the equilibrium partitioning of acrylodan-labeled heptalysines (net charge +7 and +8) onto phospholipid vesicles of defined composition. Acrylodan is a polarity-sensitive fluorescent dye with an excitation peak at 370 nm and an emission peak at 520 nm in water (Prendergast et al., 1983). When the labeled peptide binds to a membrane, the emission maximum shifts to 470 nm and fluorescence intensity increases. We determined the value of the molar partition coefficient, K, by titrating peptides with different concentrations of vesicles. We measured acrylodan fluorescence at 470 nm (slit 4 nm) and excitation at 370 nm (slit 4 nm). The fraction of the peptide bound at a given lipid concentration, $[P_b]/[P_o]$, was calculated as the ratio of the corrected fluorescence intensity of the sample to the corrected fluorescence intensity of a sample in which all of the peptide is bound to lipid. Specifically,

$$\frac{[P_b]}{[P_o]} = \frac{(F_{sample} - F_{lipid\ background}) - (F_{free\ peptide} - F_{buffer})}{(F_{all\ bound} - F'_{lipid\ background}) - (F_{free\ peptide} - F_{buffer})},$$

where $F_{free\ peptide}$ is the fluorescence at 470 nm of the peptide free in solution (a low value about equal to the fluorescence background from the buffer, F_{buffer}). K (M^{-1}) is the proportionality factor between the mole fraction of peptide bound to the membrane, χ, and the molar concentration

of peptide free in the bulk aqueous phase ($[P_f]$):

$$\chi = \frac{[P_b]}{([L] + [P_b])} = K[P_f], \quad (1A)$$

where $[P_b]$ is the molar concentration of peptide bound to the membrane and [L] is the concentration of lipid accessible to the peptide. When $[P_b] \ll [L]$, Eq. 1A may be written as

$$K = \frac{[P_b]}{[P_f][L]}. \quad (1B)$$

The total molar concentration of peptide in the solution, $[P_o]$, is the sum of bound and free peptide concentrations:

$$[P_o] = [P_b] + [P_f]. \quad (1C)$$

Combining Eqs. 1B and 1C, we obtain an expression for K as a function of known ([L]) and measured ($[P_b]/[P_o]$) quantities:

$$100\%\frac{[P_b]}{[P_o]} = \frac{K[L]}{(1 + K[L])}. \quad (1D)$$

We used Eq. 1D to fit the data in Fig. 3 *A*.

Preparation of giant vesicles for microscopy studies

We prepared giant vesicles with the gentle hydration method (Akashi et al., 1996). Briefly, 0.4–2 μmol of a 9:1 PC/PS mixture (also containing 0.3 mol% NBD-labeled PC or PS) in chloroform was dried in a V-shaped flask on a rotary evaporator under vacuum for 30 min to form a thin film. The dried film was prehydrated for 20 min at 45°C with water-saturated argon, then 5 ml of an appropriate buffer was added gently to the flask. The sealed flask was incubated for 12–24 h at 37°C. A 1-ml sample was harvested from the upper portion of the solution and used for microscopy studies. Samples containing ~40–200 μM lipid in the form of these giant, predominantly unilamellar vesicles were mixed with 1–20 μM acrylodan-labeled heptalysine, MARCKS(151–175), or, in some cases, unlabeled peptide in a small siliconized plastic tube. The mixture was transferred to a microscope slide, mixed 1:1 with agarose dissolved in buffer (0.5% w agarose) to attenuate movement of the vesicles, and covered with a coverslip.

Fluorescence digital imaging microscopy

We used a Zeiss fixed-stage Axioskop microscope and Princeton Micro-Max CCD camera to obtain images. Vesicles were imaged in fluorescence and phase-contrast mode, using a 63× oil objective. The fluorescence due to acrylodan and NBD was captured using short-band path Chroma (Chroma Technology Corp.) filter sets 31000 and 41001, respectively. For acrylodan: exciter 360 ± 20 nm, beamsplitter 400 nm, emitter 460 ± 25 nm. For NBD: exciter 460 ± 20 nm, beamsplitter 505 nm, emitter 535 ± 25 nm.

Monolayer

We used a fixed-area circular teflon trough to observe the lateral organization of 2:1 PC/PS monolayers. Acrylodan-labeled MARCKS peptide (500 nM to 2 μM) was added to the subphase after a monolayer from a 0.1 mg/ml lipid stock in chloroform was spread; the monolayer also contained 1% NBD-PS or NBC-PC. The subphase contained 10 mM KCl buffered to pH 7 with 1 mM MOPS, and the surface pressure of the monolayer was 20–30 mN/m. The monolayer was observed using a 20× long-working-distance objective.

THEORETICAL MODELS

Calculation of the zeta potential

The zeta potential was calculated using Gouy-Chapman-Stern theory (McLaughlin, 1989) and the following assumptions: 1) the membrane potential is screened only by the monovalent ions, 2) the peptides are point charges of valence +7 that bind to the membrane according to a simple linear adsorption isotherm, 3) the charges due to the acidic lipids and bound peptide are smeared uniformly over the membrane surface, and 4) the zeta potential is equal to the membrane potential at a distance of 2 Å from the membrane surface. Gouy-Chapman theory describes how the electrostatic potential, $\phi(R)$, depends on distance from the membrane surface, R:

$$\phi(R) = 2\ln\left(\frac{1 + \tanh(\phi(0)/4)\exp(-\kappa R)}{1 - \tanh(\phi(0)/4)\exp(-\kappa R)}\right), \quad (2)$$

where $1/\kappa$ is the Debye length and $\kappa = [(2kTe^2c)/(\epsilon_r\epsilon_0)]^{1/2}$; k represents the Boltzmann factor, T the absolute temperature, e the magnitude of the electronic charge, c the molar concentration of monovalent ions in the bulk, ϵ_r the dielectric constant of the aqueous phase, and ϵ_0 the permittivity of free space. The surface potential, $\phi(0)$, is given by the Gouy-Chapman-Stern equation:

$$\sinh\left(\frac{ze\phi(0)}{2kT}\right) = \frac{\sigma}{\sqrt{8NkT\epsilon_r\epsilon_0 c}\left(1 + K_{KL}c\exp\left(-\frac{e\phi(0)}{kT}\right)\right)}, \quad (3)$$

where z represents the valence of the monovalent salt ions, σ is the surface charge density, and $K_{KL} = 0.3\ M^{-1}$ is the association constant of K^+ ions with acidic lipids. σ is a sum of a negative surface charge density due to the acidic lipids in the membrane and a positive surface charge density due to membrane-adsorbed heptalysine. We assumed each lipid occupies 70 Å^2 of surface area and that the concentration of peptide bound to the membrane is given by a Henry's law adsorption isotherm.

Peptide/membrane models

Three basic peptides, acetyl-pentalysine-amide, acetyl-heptalysine-amide, and heptalysine-amide, were built in extended form using the Insight/Biopolymer molecular modeling package (INSIGHT-II; Biosym Technologies). To reduce atomic overlaps and to relax torsional and dihedral constraints, each peptide model was energy minimized using the Insight/Discover molecular modeling package (INSIGHT-II). The minimization consisted of 100 iterations with a conjugate gradient method in gas phase, using the CVFF force field and neglecting electrostatic interactions. The minimization did not significantly alter the extended structure of the peptides. The acetyl-pentalysine-amide, acetyl-heptalysine-amide, and heptalysine-amide peptide models have dimensions 17 Å × 24 Å × 7 Å, 17 Å × 31 Å × 7 Å, and 18 Å × 27 Å × 7 Å, respectively. Four different lipid bilayers, 5:1, 3:1, 2:1, and 1:1 PC/PS, were built as described by Peitzsch et al. (1995). Each lipid leaflet contains 192–432 hexagonally packed lipids, and each lipid headgroup has an area of 68 Å^2 in the plane of the membrane.

We constructed each peptide/bilayer system listed in Table 2 so that the surface-adsorbed peptides neutralized the membrane charge. These models are consistent with the zeta potential measurements (Fig. 2) and the binding measurements (Fig. 3 *B*, *open circles*), which show that the membrane charge is approximately neutralized at high concentrations of peptide. Our conclusions about discreteness effects would hold for lower concentrations of peptide as well: the electrostatic interaction free energies will be at least as strong as those listed in Table 2. In each model, the bilayer size was chosen so that the net charge of one leaflet would be neutralized by a 3 × 3 array of peptides adsorbed at the membrane surface. The peptides were distributed uniformly over the membrane surface, and each peptide in the array was placed in its approximate minimum free energy orientation. This

orientation results from the balance between the coulombic attraction and desolvation penalties, and occurs when there is ~3 Å (i.e., one layer of water) between the van der Waals surfaces of the peptide and the membrane (Fig. 1 *B*). (The exact location of these membrane-adsorbed peptides has not been determined, but several experimental studies show that small basic peptides, like pentalysine, bind to membranes outside the envelope of the polar headgroup.) A representative system used in the FDPB calculations is illustrated in Fig. 1. For the acetyl-heptalysine-amide peptide ($Z = +7$) and a 2:1 PC/PS bilayer, nine peptides (net charge +63) approximately neutralize a bilayer leaflet with 192 total lipids (net charge −64). For simplicity, we assume that the basic peptide does not produce a local redistribution of acidic lipids (Kleinschmidt and Marsh, 1997). The lateral dimensions of the bilayer are 127 Å × 113 Å; the van der Waals surfaces of adjacent peptides are separated by 25 Å in the horizontal direction and 12 Å in the vertical direction (see Fig. 1 *C*), so that each heptavalent peptide associates, on average, with seven acidic lipids. This configuration mimics an infinite peptide/membrane system: FDPB calculations performed on larger systems (5 × 5 and 7 × 7 peptide arrays) gave identical results (calculations not shown).

Finite difference Poisson-Boltzmann calculations

The peptides and lipid bilayers are represented in atomic detail and the solvent as a homogeneous medium. The univalent ions (e.g., K^+ and Cl^-) are dimensionless points, treated in the mean-field approximation. To match the experimental conditions, all calculations were performed with a monovalent salt concentration of 100 mM. The theoretical methodology is described in detail elsewhere (Ben-Tal et al., 1996); we give a brief overview below.

Each atom of the peptides and bilayer is assigned a radius and partial charge that is located at its nucleus; the peptide/membrane model is then mapped onto a three-dimensional lattice of l^3 points, each of which represents a small region of the peptide, membrane, or solvent. The charges and radii used for the amino acids were taken from a CHARMM22 parameter set (Brooks et al., 1983); those used for the lipids are the ones described by Peitzsch et al. (1995) and were used in previous studies (Ben-Tal et al., 1996, 1997; Murray et al., 1998). Smooth molecular surfaces for the peptides and membrane are generated by rolling a spherical probe with the radius of a water molecule (1.4 Å) over the surfaces defined by the van der Waals radii of the constituent atoms; the point of contact between the probe and the van der Waals surface defines the molecular surface. Lattice points that lie within the molecular surfaces of the peptides and bilayer are assigned a low dielectric constant (2), and lattice points outside the molecular surfaces, corresponding to the aqueous phase, are assigned a high dielectric constant (80). Salt ions are excluded from a region that extends 2 Å (the radius of a Na^+ ion) beyond the van der Waals surfaces of the peptide and membrane. The electrostatic potential and the mean distribution of the monovalent salt ions at each lattice point are calculated by solving the nonlinear Poisson-Boltzmann equation:

$$\nabla[\epsilon(r)\nabla\phi(r)] - \epsilon_r\kappa(r)^2\sinh(\phi(r)) + \frac{e^2}{\epsilon_o kT}\rho^f(r) = 0, \qquad (4)$$

where $\epsilon(r)$ is the dielectric constant, $\phi(r)$ is the electrostatic potential, and $\rho^f(r)$ is the charge density of the fixed charges. Equation 4 is mapped onto the cubic lattice and solved for $\phi(r)$, using the finite-difference approximation and the quasi-Newton method (Holst, 1993), combined with three levels of multigriddings (Holst and Saied, 1993).

A sequence of focusing runs of increasing resolution is employed to calculate the electrostatic potentials. In the initial calculation, the peptide/membrane model fills a small percentage of the lattice (~10%), and the potentials at the boundary points of the lattice are approximately zero. This procedure ensures that the system is electroneutral. To mimic an infinite membrane, periodic boundary conditions in the directions that span the membrane plane are applied when the bilayer spans less than 100% of the lattice. The solutions of the Poisson-Boltzmann equation (Eq. 4) are used to calculate the electrostatic free energy of the system. For the case of a peptide interacting with a membrane in the absence of other peptides, the electrostatic free energy of interaction is the difference between the electrostatic free energy when the peptide associates with the membrane and the electrostatic free energy when the peptide and the membrane are an infinite distance apart. For the case of a peptide interacting with a membrane in the presence of other peptides, the calculation is the same, except that the other eight peptides of the 3 × 3 array are fixed at the membrane surface (see Fig. 1 *D*).

The lattice size and final resolution used to calculate the electrostatic free energies depend on the size of the peptide/membrane model. For example, the FDPB calculations for the scenario illustrated in Fig. 1 were performed with a lattice size of $l = 209$ and a series of focusing runs with resolutions of 0.2, 0.4, 0.8, and 1.6 grid/Å. The electrostatic free energy of interaction between the central peptide and the membrane, in both the presence and absence of other peptides, differed by less than 0.1 kcal/mol between the 0.8 and 1.6 grid/Å scales when the van der Waals surfaces of the peptide and membrane were separated by 3 Å. In performing the calculations summarized in Table 2 and Fig. 4, we used lattice sizes of $l =$ 209–289 and final resolutions of 1.2–2.0 grid/Å; in all cases, the electrostatic free energy of interaction differed by less than 0.25 kcal/mol between the two highest resolution scales.

Previous work showed that we can predict correctly how the membrane binding of a basic peptide depends on the mole percentage of acidic lipid in the membrane, the ionic strength of the solution, or the number of basic residues in the peptide by considering a single orientation of the peptide with respect to the membrane, specifically, the orientation of minimum free energy in which the peptide's potential interacts maximally with the membrane potential (Ben-Tal et al., 1996). Here we exploit this simplification to predict how the membrane binding of a basic peptide depends on the surface concentration of peptide by calculating the difference between the electrostatic free energies of interaction between the peptide, in its minimum free energy orientation, and the membrane in the presence and absence of the other surface-adsorbed peptides.

RESULTS

Experimental measurements

The effect of heptalysine on the zeta potential of PC/PS vesicles suggests that discreteness-of-charge effects are important

Fig. 2 shows how changing the aqueous concentration of heptalysine affects the zeta potential of 2:1 PC/PS LUVs in 100 mM monovalent salt. The zeta potential, ζ, is calculated from the measured value of the electrophoretic mobility, u, the velocity of a vesicle in a unit electric field, using the Helmholtz-Smoluchowski equation (Hunter, 1981):

$$\zeta = u\eta/(\epsilon_r\epsilon_o), \qquad (5)$$

where η is the viscosity of the aqueous solution, ϵ_r is the dielectric constant of the aqueous solution, and ϵ_o is the permittivity of free space. The filled circles in Fig. 2 show that the zeta potential of 2:1 PC/PS vesicles varies linearly with the logarithm of heptalysine concentration; the slope is 14.5 mV per decade. This slope is significantly steeper than the 6.0 mV per decade predicted using the smeared charge treatment given in Eqs. 2 and 3. The maximum theoretical value for the slope, within the context of smeared charge Gouy-Chapman theory, is obtained from Eq. 3 by assuming 1) the potential is very negative, 2) the plane of shear is at the vesicle surface, 3) monovalent ions can be ignored, and 4) the peptides exert only a screening effect; the simple

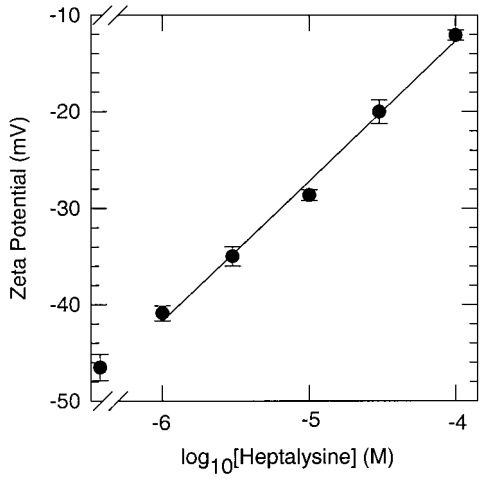

FIGURE 2 The effect of heptalysine (acetyl-heptalysine-amide, valence $Z = 7$) on the zeta potential of 2:1 PC/PS vesicles. The aqueous solution contained 100 mM KCl buffered to pH 7.0 with 1 mM MOPS at 25°C. Each filled circle represents the average of ≥30 measurements ± SD (four separate experiments). The line is the least-squares best fit through the experimental points; it has a slope of 14.5 mV per decade of peptide concentration. Gouy-Chapman-Stern theory predicts a slope of 6.0 mV per decade (see text).

Gouy equation then predicts the slope is $2.3kT/Ze \sim 59/Z$ mV/decade (at $T = 25$°C). For a peptide with a valence of $Z = +7$, the maximum slope predicted by smeared charge theory is thus $59/7 = 8.4$ mV per decade, substantially less than the experimentally measured value of 14.5 mV per decade.

The simplest explanation for the disparity between the observed (Fig. 2) and predicted change in potential relates to the discrete nature of the net charge on the adsorbing peptide; a disparity could arise if each adsorbing basic peptide senses a local potential significantly more negative than the average potential, as illustrated in Fig. 1. The net effect is that more peptides adsorb to the surface, producing larger changes in the zeta potential. In the Appendix, we investigate experimentally the possibility that high concentrations of basic peptides produce large lateral domains enriched in acidic lipids and peptide; our results suggest that heptalysine does not produce such domains.

High concentrations of unlabeled heptalysine decrease the membrane association of acrylodan-labeled heptalysine much less than predicted by smeared charge theory

Table 1 illustrates the effect of high concentrations of unlabeled heptalysine on the membrane association of acrylodan-labeled heptalysine. (The binding of an acrylodan-labeled heptalysine (acetyl-heptalysine-(cysteine-acrylodan)-amide, $Z = 7$, $K = 6 \times 10^4$ M^{-1}) is 100-fold stronger than the binding of the unlabeled heptalysine (acetyl-heptalysine-amide, $Z = 7$, $K = 6 \times 10^2$ M^{-1}) to 5:1 PC/PS(PG) vesicles (data not shown), presumably because of the hydrophobic insertion of the acrylodan label into the membrane interface.) In the absence of unlabeled peptide, acrylodan-heptalysine binds to 5:1 PC/PS vesicles in 100 mM KCl with a molar partition coefficient $K = 6.8 \times 10^4$ M^{-1}. Adding 100 μM unlabeled heptalysine decreases K less than twofold and changes the zeta potential of the vesicles by 13 mV (from −33 to −20 mV; data not shown). This potential change should be a good approximation for the change in the average surface potential ($\Delta\zeta \approx \Delta\phi(0)$). If we use this average or smeared charge potential in the Boltzmann relation, it predicts a much larger (40-fold) decrease in the membrane association than is observed. The simplest explanation for this discrepancy is the discreteness of charge effect illustrated in Fig. 1: the effect of unlabeled heptalysine on the membrane association of acrylodan-labeled heptalysine is less than predicted by smeared charge theory because the labeled peptide experiences a local potential more negative than the average potential.

TABLE 1 The effect of acetyl-heptalysine-amide on the binding of 50 nM acetyl-heptalysine-(cysteine-acrylodan)-amide ($Z = +7$) to 5:1 PC/PS 100 nm vesicles in 100 mM KCl, 1 mM MOPS, pH 7

[Acetyl-heptalysine-amide] (μM)	K (M^{-1})
0	6.8×10^4
1	6.7×10^4
5	6.3×10^4
100	4.2×10^4

K is the molar partition coefficient of the fluorescently labeled peptide as determined by Eq. 1D from measurements similar to those illustrated in Fig. 3*A*. The estimated accuracy of K is ±20%.

The membrane association of acrylodan-labeled heptalysine depends on how the net charge density of the membrane is changed

We examined the membrane association of acrylodan-labeled heptalysine ($Z = +8$) as a function of net charge density on the vesicles. (The results of Fig. 3 were obtained with a peptide in which cysteine was placed at the N-terminus and subsequently labeled with acrylodan as described in Materials and Methods. The C-terminus was amidated, but the N-terminus was left unblocked, resulting in a peptide of valence +8. Data qualitatively similar to those in Fig. 3 were obtained with an acrylodan-labeled heptalysine (acetyl-heptalysine-(cysteine-acrylodan)-amide) with a valence of $Z = +7$.) We manipulated the vesicle charge density by either varying the mole percentage of acidic lipid in the vesicles in the limit of low peptide concentration or adding high concentrations of peptide to vesicles of fixed lipid composition.

Fig. 3 *A* plots the percentage peptide bound as a function of lipid concentration for 5:1, 8:1, 15:1, or 25:1 PC/PS vesicles. The curves are the least-squares best fits to the molar partition equation (Eq. 1D). Fig. 3 *A* illustrates that reducing the negative charge density of the vesicles by decreasing the acidic lipid from 17 to 4 mol% decreases the molar partition coefficient ~1000-fold. The filled circles in

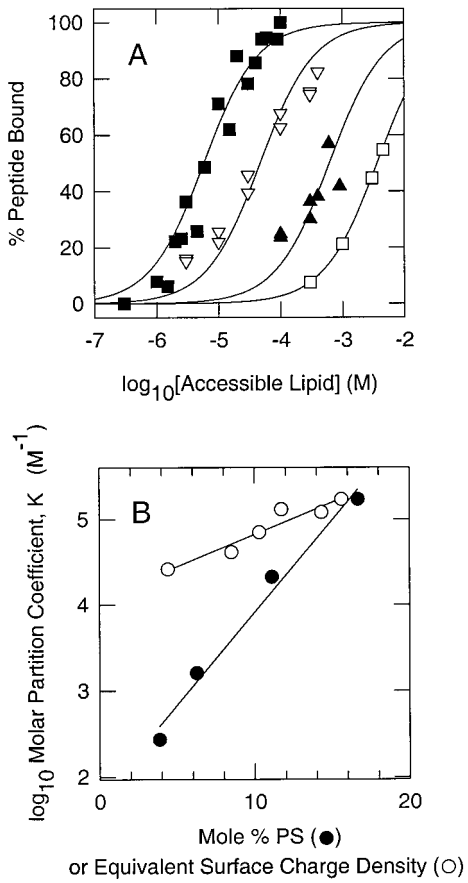

FIGURE 3 (*A*) Binding of acrylodan-labeled heptalysine (acrylodan-cysteine-heptalysine-amide, $Z = 8$) to PC/PS vesicles depends markedly on the mole percentage PS in the vesicle. The percentage peptide bound to the vesicles is plotted against the concentration of accessible lipid (1/2 the total lipid concentration for 100-nm large unilamellar vesicles) for 5:1 (■), 8:1 (▽), 15:1 (▲), and 25:1 (□) PC/PS vesicles. The concentrations of peptide were too low to affect the surface charge of the vesicles significantly: 20 nM (5:1 PC/PS vesicles), 100 nM (8:1 and 15:1), and 200 nM (25:1). The aqueous solutions also contained 100 mM KCl buffered to pH 7.0 with 1 mM MOPS. The curves illustrate the least-squares best fit of Eq. 1D to the data. The molar partition coefficient, *K*, is determined from this fit: *K* is the reciprocal of the lipid concentration that produces half-maximum binding. (*B*) The partition coefficient of acrylodan-labeled heptalysine depends upon how the surface charge density of the membrane is changed. ●, Plot of the molar partition coefficient, as determined from the data in *A*, as a function of the mole percentage PS in the PC/PS vesicles. A 4-fold decrease in surface charge density produces a 1000-fold decrease in *K*. ○, Plot of the molar partition coefficient, as determined from experiments similar to those illustrated in *A*, as a function of the equivalent surface charge density of the membrane (defined as the mole percentage PS that will produce the same average charge per area). The equivalent surface charge density is determined by assuming all fixed charges (from both the acidic lipids and adsorbed peptides) at the membrane surface are smeared uniformly over the surface. The vesicles were formed from 5:1 PC/PS. In this case a 4-fold decrease in the surface charge density produces only a 5-fold decrease in *K*.

Fig. 3 *B* show the data in Fig. 3 *A* plotted as a function of the average surface charge density of the vesicles expressed as the mole percentage of acidic lipid in the vesicle. Both the FDPB calculations and Gouy-Chapman-Stern theory predict a 1000-fold reduction in membrane association of heptalysine as the mole percentage of acidic lipid decreases from 17 to 4 (calculations not shown; see figure 7 of Ben-Tal et al., 1996, for calculations with pentalysine), indicating that smeared charge theory describes adequately the membrane association of simple basic peptides in the limit of low peptide concentration. This steep dependence of membrane association on the mole percentage of acidic lipid has been observed with other basic peptides, e.g., the pseudo-substrate region of protein kinase C (Mosior and McLaughlin, 1991), the effector region of MARCKS (Kim et al., 1994), the N-terminal region of Src (Buser et al., 1994), the C-terminus of K-Ras (Ghomashchi et al., 1995; Leventis and Silvius, 1998), and pentalysine (Kim et al., 1991; Ben-Tal et al., 1996). (Insertion of alanines between lysines in a heptalysine decreases the binding. Specifically, the molar partition coefficients onto 4:1 PC/PS vesicles are $\sim 5 \times 10^5\ M^{-1}$ for acrylodan-labeled CK_7-amide, $1.6 \times 10^5\ M^{-1}$ for acrylodan-labeled $CK(AK)_6$-amide, and $6 \times 10^4\ M^{-1}$ for acrylodan-labeled $CK(AAK)_6$-amide peptides. This result agrees well with the published data on pentalysine and pentaarginine peptides with one or two alanines between the basic residues (Mosior and McLaughlin, 1992).)

We also changed the average charge density on the membrane by varying the concentration of peptide in a solution with 5:1 PC/PS vesicles. Using measurements similar to those illustrated in Fig. 3 *A* (data not shown), we determined the concentration of lipid required to produce half-maximum binding at total peptide concentrations of 20, 50, 100, 200, 500, 1000 nM acrylodan-heptalysine. The reciprocal of this lipid concentration is (theoretically within 10% under our conditions) the molar partition coefficient. At high concentrations of peptide, *K* in Eq. 1D is a function of the number of peptides bound per unit area of membrane, which decreases as the lipid concentration increases for a constant peptide concentration. We calculated an average surface charge density at each (half total bound) peptide concentration by assuming the charges from the bound peptide and acidic lipids are smeared uniformly on the surface of the vesicles. Increasing the total concentration of peptide from 20 to 1000 nM produces a change in average surface charge density comparable to decreasing the acidic lipid content of the vesicles from 17 to 4 mol% (Fig. 3 *B*, *open and filled circles*). Note that the decrease in membrane association of the peptide is much smaller when the change in vesicle charge density is due to an increase in the peptide concentration; we observed only a 5-fold decrease in membrane association when the peptide concentration was increased from 20 to 1000 nM (*open circles*) compared to the 1000-fold decrease due to decreasing the acidic lipid from 17 to 4 mol% (*filled circles*). While smeared charge theory accurately describes the membrane association as a function of mole percentage of acidic lipid, it cannot account for the results obtained by varying the peptide concentration. This indicates that the charges in the system cannot all be treated equally; it is necessary to account for the discrete nature of

the peptide to describe its membrane association at high concentrations. The "discreteness-of-charge" effect illustrated in Fig. 1 arises from the localized effect of the peptide charge on the membrane potential and could account for the lower dependence of membrane association on peptide concentration that we observe.

High concentrations of basic peptide can reverse the charge of PS and PC/PS vesicles

It follows, as a corollary of the discreteness-of-charge effect illustrated in Fig. 1, that sufficiently high concentrations of basic hydrophilic peptides should reverse the charge on a PC/PS or PS vesicle. Extrapolation of the line in Fig. 2, for example, suggests that 10^{-2} M heptalysine should produce a zeta potential of +15 mV on a 2:1 PC/PS vesicle. Unfortunately, this experiment is prohibitively expensive. We examined instead the effect of poly-L-lysine (average molecular weight 1000) on the zeta potential of PC, 2:1 PC/PS, and PS vesicles formed in a 0.1 M KCl, 1 mM MOPS, pH 7.0 solution. As expected, addition of 10^{-4} M peptide had no effect on the (approximately zero) zeta potential of the PC vesicles but reversed the sign of the zeta potentials of the PC/PS and PS vesicles to $+22 \pm 1$ ($n = 20$) mV and $+30 \pm 2$ ($n = 20$) mV, respectively.

Theoretical calculations

Calculations with atomic models provide a molecular basis for the discreteness-of-charge effects observed with peptide/membrane systems

The experimental results reported here suggest that discreteness-of-charge effects are important when high concentrations of basic peptides bind to membranes. The FDPB calculations depicted in Fig. 1 can account qualitatively for our experimental observations. Each peptide perturbs the membrane potential in a highly localized manner. Adsorption of enough heptalysine to effectively neutralize the negative surface charge of the membrane produces a nonuniform pattern of negative and positive local potential that can lead to attractive electrostatic interactions between the peptide and the membrane, even though the average potential at the membrane surface is zero. This is examined in more detail below.

The electrostatic free energy of interaction between a basic peptide and the membrane depends weakly on the presence of other surface-adsorbed peptides

Fig. 1 illustrates the results of FDPB calculations we performed for one scenario: the electrostatic interaction of heptalysine with a 2:1 PC/PS bilayer in 100 mM KCl in the presence or absence of other surface-adsorbed peptides. We performed similar calculations using a range of membrane compositions (5:1, 3:1, 2:1, 1:1 PC/PS) and peptide valences (acetyl-pentalysine-amide, $Z = +5$; acetyl-heptalysine-amide, $Z = +7$; heptalysine-amide, $Z = +8$). We constructed uniform peptide arrays that effectively neutralized the net negative surface charge of the membrane (i.e., one $+Z$-valent peptide per Z acidic lipids) and calculated the total electrostatic free energy of the peptide/membrane systems by solving the FDPB equation numerically as described in Materials and Methods.

Table 2 summarizes our results; in all cases, the electrostatic interaction between the peptide and membrane in the presence of other peptides is almost as strong as the interaction in the absence of other peptides. The difference between the interaction free energies in the two cases increases with increasing mole percentage of acidic lipid because the surface density of peptide required to neutralize the membrane charge and hence the peptide-peptide repulsion increases. The relatively small differences predicted for 5:1, 3:1, and 2:1 PC/PS membranes (<1 kcal/mol; Table 2) suggest there should be only a small decrease in the membrane partitioning upon the addition of high peptide concentrations, as was observed experimentally (Table 1 and Fig. 3).

A uniform arrangement of peptides in an array at the membrane surface maximizes the discreteness of charge effects (Fig. 1 *C*), so we examined deviations from uniformity by sampling different positions of the peptide at the center of the array while keeping the other peptides fixed. The results shown in Fig. 4 indicate that our calculations are not overly sensitive to the exact orientation of the central peptide. First, we calculated the electrostatic free energy of interaction of the central peptide with the membrane as a function of its position (x, y) in the plane of the array. Fig. 4 *A* shows that the potential well experienced by the peptide is quite broad. The central peptide in Fig. 1 *C* was moved along the horizontal direction ($y = 0$) from $x = -25$ Å to $x = +25$ Å, the positions at which its van der Waals surface is just touching the van der Waals surface of a peptide on either side; $x = 0$ Å corresponds to the position in the center of the array. The interaction free energy does not change appreciably until the van der Waals surface of the central

TABLE 2 Summary of FDPB calculations of the electrostatic free energy of interaction between the central peptide and a membrane in the absence ("no peptide") and presence ("neutralizing array") of other surface-adsorbed peptides

	Electrostatic free energy of interaction (kcal/mol)			
	5:1 PC/PS	3:1 PC/PS	2:1 PC/PS	1:1 PC/PS
Lys_5: no peptide	−2.6	−4.2	−4.7	−5.7
Lys_5: neutralizing array	−2.4	−3.7	−3.8	−4.4
Lys_7: no peptide	−3.3	−5.1	−6.5	−7.9
Lys_7: neutralizing array	−3.3	−4.6	−5.8	−6.4
Lys_7 ($Z = 8$): no peptide	−4.2	−5.7	−7.7	−9.4
Lys_7 ($Z = 8$): neutralizing array	−3.9	−5.3	−7.9	−7.6

All calculations were performed with 100 mM monovalent salt. Lys_5 = acetyl-pentalysine-amide; Lys_7 = acetyl-heptalysine-amide; Lys_7 ($Z = 8$) = hepatlysine-amide.

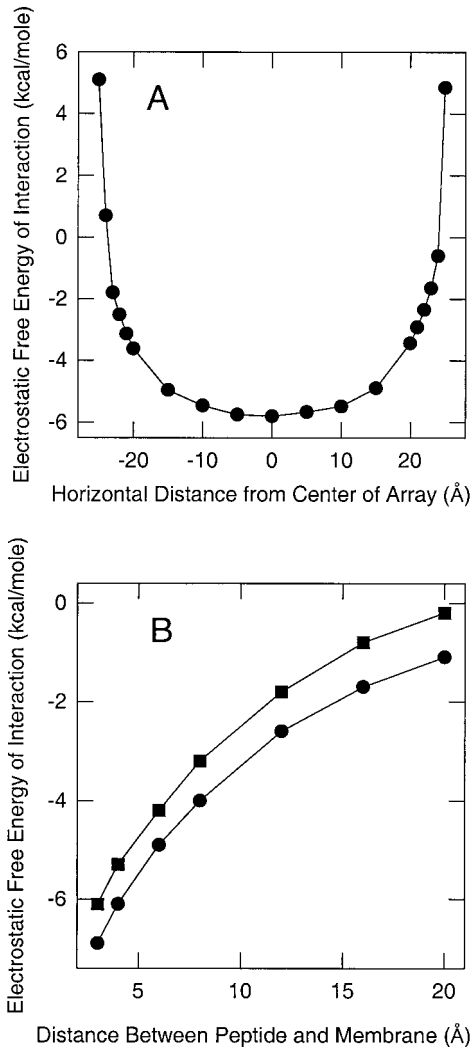

FIGURE 4 Electrostatic free energy of interaction as a function of peptide position. The FDPB calculations were performed on the system illustrated in Fig. 1 *C*: a 2:1 PC/PS membrane in 100 mM KCl with enough adsorbed heptalysine to neutralize the negative surface charge of the membrane. (*A*) The electrostatic free energy of interaction between the central peptide and the membrane in the presence of the other peptides, whose positions remained fixed, was calculated as the position of the central peptide was varied horizontally from $x = -25$ Å, where its van der Waals surface just touches the van der Waals surface of the peptide on the left, to $x = +25$ Å, where its surface just touches the surface of the peptide on the right. The electrostatic free energy of interaction calculated at $x = 0$ Å (the center of the array) corresponds to the value reported in Table 2. (*B*) The electrostatic free energy of interaction as a function of height above the membrane surface. The electrostatic free energy of interaction between the central peptide and the membrane in the absence (●) and presence (■) of the other peptides, the positions of which remained fixed, was calculated as the height of the central peptide (R) varied from 3 Å to 20 Å.

peptide is within ~10 Å (one Debye length in 100 mM KCl) of the van der Waals surface of a peptide on either side ($|x| \approx 15$ Å). The repulsive peptide-peptide interaction increases sharply for $|x| > 15$ Å but does not overcome the favorable peptide-membrane interaction until $|x| \approx 23$ Å, where the peptides' van der Waals surfaces are separated by only 2 Å. Similar results were obtained along different directions in the plane of the array and for other conditions listed in Table 2 (calculations not shown). Next we calculated the electrostatic free energy of interaction of the central peptide with the membrane as a function of its height, R, above the membrane surface. Fig. 4 *B* shows that the central peptide senses a significant negative potential out to $R \approx 15$ Å (1½ Debye lengths in 100 mM KCl). The squares (circles) in Fig. 4 *B* represent the electrostatic free energy of interaction in the presence (absence) of other peptides fixed at the membrane surface. The difference between the interaction free energies in the presence or absence of surface-adsorbed peptides is relatively small (<1 kcal/mol) and increases slightly with increasing height above the membrane surface. The calculations in Fig. 4 *B* suggest that a peptide in the aqueous phase can be attracted electrostatically to the membrane surface, even when the surface density of bound peptide is sufficiently high to neutralize the membrane surface charge.

DISCUSSION

We examined experimentally the association of heptalysine with PC/PS vesicles under conditions of high peptide concentrations and obtained three types of results that suggest that discreteness-of-charge effects are important. First, as the heptalysine concentration in the aqueous phase increases, the zeta potential of 2:1 PC/PS vesicles increases more rapidly than predicted by smeared charge theory (Fig. 2). Similar results were observed previously with other simple basic peptides (Mosior and McLaughlin, 1991; Kim et al., 1991, 1994). Second, acrylodan-heptalysine binds more strongly to 5:1 PC/PS vesicles in the presence of high concentrations of unlabeled peptide (Table 1) than predicted by smeared charge theory. More revealingly, the decrease in membrane association of acrylodan-labeled heptalysine depends dramatically on whether the net surface charge density of the vesicles is changed by varying the mole percentage of acidic lipid or by varying the amount of peptide bound (Fig. 3). We found that the membrane partitioning of acrylodan-labeled heptalysine at low peptide concentrations is a steep function of mole percentage of monovalent acidic lipid; the binding decreases 1000-fold as the mole percentage of acidic lipid is decreased from 17% to 4%. In contrast, changing the effective surface charge density of 5:1 PC/PS vesicles over the same range by increasing the amount of adsorbed peptide decreases the membrane association only 5-fold (Fig. 3). Third, basic peptides can reverse the zeta potentials of PC/PS and PS vesicles. These results and our FDPB calculations suggest that discreteness-of-charge effects are important for describing nonspecific electrostatic interactions between basic peptides and membranes. Specifically, our calculations with atomic models of peptides and membranes (Fig. 1 and Table 2) show that a peptide adsorbing to a membrane when the peptide concentration is high experiences a local potential significantly more negative than the average, smeared charge potential.

The FDPB methodology has been used successfully to describe the membrane association of pentalysine, charybdotoxin and its analogs, and peptides corresponding to the N-terminus of Src in the limit of low peptide concentration (Ben-Tal et al., 1996, 1997; Murray et al., 1998). The methodology makes a number of simplifying assumptions (e.g., the peptide and membrane are static structures, and the aqueous phase is treated as a structureless medium) that have been discussed in detail elsewhere (Ben-Tal et al., 1996), but it describes well the long-range electrostatic attraction that is the main component of the membrane association of these peptides. Previous work described how to calculate the molar partition coefficient of peptide onto membrane under conditions where peptide-peptide interactions can be ignored (Ben-Tal et al., 1996). In this report, we provide a detailed model of the electrostatic interactions between peptide and membrane when the surface concentration of peptide is high, but we make no attempt to calculate the partition coefficient under these conditions. Other groups have used statistical thermodynamics to construct adsorption isotherms that describe the membrane association of peripheral peptides under conditions where interactions between the surface-adsorbed peptides are important (Heimburg and Marsh, 1995; Chatelier and Minton, 1996; Heimburg et al., 1999). The treatments account for the entropy of the surface distribution of peptide (e.g., through area exclusion models) and nonelectrostatic interactions between the surface-adsorbed peptides, but the electrostatic interactions between the peptides and the membrane have been treated in the context of smeared charge theory. It should be possible to combine the FDPB and statistical thermodynamic methodologies to deduce the full membrane binding isotherm when lateral interactions at the membrane surface are significant.

Biological significance

The cytoplasmic leaflet of the plasma membrane of a typical mammalian cell has 20–30 mol% monovalent acidic lipid and contains lateral domains enriched in proteins with surface-adsorbed basic clusters. For example, MARCKS associates with the plasma membrane through a combination of hydrophobic and electrostatic interactions mediated by its myristate and basic effector region, respectively (McLaughlin and Aderem, 1995; Seykora et al., 1996; Swierczynski and Blackshear, 1996); it has a punctate distribution in the plasma membrane of macrophages (Rosen et al., 1990). The cellular concentration of MARCKS is sufficiently high ($\sim$10 μM) that we expect the MARCKS-rich regions of the plasma membrane, the nascent phagosomes, to be effectively neutralized by the cluster of 13 basic residues in the effector region. The local potential effect illustrated in Fig. 1 *C* could account for the colocalization of other proteins whose membrane association also requires electrostatic interaction with acidic lipids. For example, protein kinase C α (PKC) colocalizes with MARCKS in nascent phagosomes (Allen and Aderem, 1995); electrostatic interactions of the Ca^{2+}-bound C2 domain of PKC with acidic lipids contribute to its membrane localization (Rizo and Sudhof, 1998; Newton and Johnson, 1998).

Our experimental results support the suggestion, illustrated in Fig. 1, that the electrostatic potential is highly nonuniform at the surface of a membrane containing acidic lipids and adsorbed basic peptides (or proteins with membrane-adsorbed clusters of basic residues). Fig. 1 *C* illustrates that the localized areas of positive potential could act as basins of attraction for multivalent acidic lipids present at trace concentrations in the plasma membrane. Specifically, the trivalent (Toner et al., 1988) acidic lipid phosphatidylinositol-4,5-bisphosphate (PIP_2), an important source of second messengers in cells, should partition nonspecifically into these regions because the Boltzmann relation predicts that its local concentration depends on the cube of the local potential. The lateral accumulation of PIP_2 due to nonspecific electrostatic interactions could act in combination with specific protein-lipid interactions (Martin, 1998). Thus our theoretical model (Fig. 1) suggests that PIP_2 should be sequestered with MARCKS in nascent phagosomes of macrophages, with AKAP79 in the postsynaptic region of neurons, with the basic membrane-anchored C-terminus of the synaptic fusion complex (Sutton et al., 1998), and with caveolin/neuromodulin/eNOS (which all have clusters of basic residues) in caveolae/detergent-resistant membranes (DRMs). Currently, it is not known whether PIP_2 is accumulated with MARCKS or AKAP79, but PIP_2 is required for exocytosis (Martin, 1998), and several recent reports suggest that PIP_2 is sequestered in caveolae/DRMs (Liu et al., 1997; Liu et al., 1998).

APPENDIX: DO BASIC PEPTIDES FORM LARGE LATERAL DOMAINS WITH ACIDIC LIPIDS WHEN THEY BIND TO PHOSPHOLIPID VESICLES?

Several studies have reported that basic peptides (e.g., the MARCKS effector region peptide, MARCKS(151–175), and pentalysine) appear to induce the formation of large (>1 μm) lateral domains enriched in acidic lipids when they bind to PC/PS giant unilamellar vesicles (Yang and Glaser, 1995, 1996; Glaser et al., 1996; Denisov et al., 1997; Epand et al., 1998). In brief, fluorescence digital microscopy by Glaser and colleagues showed that before the addition of peptide the NBD-PS fluorescence was uniform over the PC/PS vesicle, but that after the addition of peptide, regions of enhanced NBD-PS fluorescence appeared; these regions of enhanced NBD-PS fluorescence colocalized with regions of enhanced fluorescence due to the acrylodan-labeled peptide. We confirmed these observations and extended them to acrylodan-labeled heptalysine (data not shown for any of the results reported in this Appendix). These results appear to support the hypothesis that basic peptides produce redistribution of PS into large lateral domains when they bind to PC/PS vesicles. We report here, however, the results of three control experiments that suggest that the formation of these putative lateral domains is not due to lateral reorganization of the acidic lipids and peptides on the surface of a single vesicle but is more likely due to peptide-induced aggregation of vesicles.

We first note that several types of experiments (e.g., light scattering, direct observation under a microscope) show that MARCKS(151–175), pentalysine, and heptalysine produce extensive vesicle aggregation under conditions where they induce the formation of putative lateral domains.

(Aggregation is not unexpected under these conditions because the formation of putative domains is observed only when sufficient peptide is adsorbed to the vesicle to essentially neutralize the charge on the vesicle.) A typical sample of giant unilamellar vesicles we used contained 25–100 μM lipid (9:1 PC/PS). Before the addition of peptide, $<$10% of the vesicles were in obvious aggregates, as revealed by direct microscopic observation; addition of basic peptides induced aggregation of the vesicles. For example, in a sample with 2–5 μM MARCKS(151–175) peptide, 20–30% of vesicles were in obvious aggregates; these aggregated vesicles were ignored. Of the remaining, apparently unaggregated vesicles, ~80–90% had putative domains; the other 10–20% had an apparently uniform distribution of NBD-PS and adsorbed acrylodan-labeled peptide (30–50 apparently unaggregated vesicles were studied in each experimental condition).

The following three control experiments suggest that the putative lateral domains may actually result from the peptide-induced aggregation of vesicles. First, each time we observed a putative lateral domain in fluorescence mode we saw a colocalized region of extra darkness in phase-contrast mode. (These measurements were made with the same objective, a Zeiss Plan-Neofluar (63$\times$ oil, Ph 3), which allowed rapid switching between fluorescence and phase-contrast modes.) The simplest explanation of this result is that the extra layer of darkness in phase comes from an extra layer (or layers) of lipid bilayer. The extra membrane could be due to the aggregation then collapse/explosion and flattening of a second giant unilamellar vesicle (or to the aggregation of many small secondary vesicles) on the primary vesicle under observation. Four additional experiments argue against the possibility that the region of extra darkness in phase came from absorption of light: 1) Vesicles with labeled and unlabeled lipids displayed the same darkness in phase contrast (when no peptides were present). 2) Vesicles with acrylodan-labeled peptide but no putative domains had no extra darkness in phase. 3) Photobleaching both the peptide and the lipid labels while putative domains were under observation did not change the extra darkness visible in the phase-contrast image. 4) Putative domains induced by unlabeled peptide (or observed with labeled peptide and unlabeled lipid) also had an extra dark region in phase-contrast mode.

Second, if the enhanced NBD-PS fluorescence from putative lateral domains were indeed due to lateral segregation of the acidic PS lipids with peptides in the PC/PS vesicles, the NBD-PC fluorescence from the domain should have decreased, or at least not increased to the same degree as the NBD-PS fluorescence. Thus we conducted parallel experiments with NBD-PC (or Bodipy-PC, which we used because there is less energy transfer between acrylodan and Bodipy than NBD) instead of NBD-PS. We observed about the same two- to fourfold enrichment of NBD-PC (Bodipy-PC) or NBD-PS fluorescence in putative domains induced by either acrylodan-labeled MARCKS(151–175) or heptalysine. The similar enrichment of both fluorescent PC and PS in a putative domain area suggests that lateral reorganization of acidic lipids is not responsible for the phenomenon.

Third, there was no detectable peptide-induced lateral domain formation in a 2:1 PC/PS monolayer containing either 1 mol% NBD-PS or NBD-PC (or in a 9:1 PC/PS supported bilayer) upon the addition of peptide (e.g., acrylodan-labeled MARCKS(151–175)). NBD-PS appeared to be distributed homogeneously before and after the addition of peptide, which also displayed homogeneous fluorescence. Monolayers are not identical to bilayers, but large lateral domains can be observed in monolayers under other conditions (Möhwald, 1990; McConnell, 1991). Specifically, we could observe lateral domains formed in monolayers formed from cholesterol/SM/PC mixtures, using 1 mol% NBD-PC or NBD-PS as a probe, in agreement with recent epifluorescence studies (e.g., Keller et al., 1998). Our inability to detect large lateral domains on monolayers after the addition of basic peptides to the subphase thus supports the conclusion from the experiments described above that the putative domains observed on vesicles upon the addition of basic peptides are probably not due to the lateral reorganization of acidic lipids. This conclusion is also consistent with the results of a recent study that measured the electrostatic binding of negatively charged macromolecules to membranes containing positively charged lipids. Direct microscopic observations of individual fluorescently labeled DNA molecules bound to supported bilayer membranes indicate that large lateral domains do not form as the DNA concentration increases (Maier and Rädler, 1999).

Our previous observation that MARCKS(151–175) inhibits PLC activity (Glaser et al., 1996) also probably reflects vesicle aggregation rather than the formation of authentic large lateral domains that sequester PIP_2. Specifically, the MARCKS(151–175)-induced PLC inhibition always correlated with aggregation of the vesicles; release of PLC inhibition by phosphorylation of MARCKS(151–175) or the addition of Ca^{2+}-calmodulin causes the MARCKS(151–175) peptide to desorb from the vesicles, reversing vesicle aggregation.

The simplest explanation for these results is that the putative large lateral domains induced by basic peptides such as pentalysine, heptalysine, and MARCKS(151–175) are actually due to peptide-induced vesicle aggregation, probably followed by collapse/explosion of the secondary vesicle onto the surface of the primary vesicle. Of course, our results do not rule out the existence of authentic peptide-induced lateral domains (we have not conducted experiments to search for submicroscopic lateral domains, such as those considered by Mouritsen and Jørgensen (1997)), and other explanations of our results are possible. For example, the peptide-induced formation of large lateral domains consisting of submicroscopic "microvilli" could explain our vesicle results, but this bilayer couple mechanism seems unlikely, if only because there is good evidence that pentalysine and heptalysine do not penetrate the polar headgroup region of the bilayer. In our opinion, future studies that address the question of peptide-induced domain formation should be conducted on systems that do not suffer from possible aggregation artifacts, e.g., monolayers, single supported bilayers, and large single vesicles isolated from other vesicles before the addition of peptides (Kwok and Evans, 1981; Needham, 1993).

This work was supported by National Science Foundation grant MCG-9729538 and National Institutes of Health grant GM24971 to SM, by National Science Foundation grant MCB-9808902 to BH, by Israel Science Foundation grant 683/97 and fellowships from the Wolfson and Alon Foundations to NB-T, and by a Helen Hay Whitney Postdoctoral Fellowship to DM. The calculations were carried out on the Origin2000 at the National Center for Supercomputing Applications (University of Illinois at Urbana-Champaign) under grant MCA95C015, on the CRAY C90 at the Pittsburgh Supercomputing Center under grant MCB980011P, and on the CRAY J91 and DEC Alpha at the Frederick Biomedical Supercomputing Center at the Frederick Cancer Research and Development Center.

REFERENCES

Akashi, K., H. Miyata, H. Itoh, and K. Kinosita, Jr. 1996. Preparation of giant liposomes in physiological conditions and their characterization under an optical microscope. *Biophys. J.* 71:3242–3250.

Allen, L. A., and A. Aderem. 1995. A role for MARCKS, the α isozyme of protein kinase C and myosin I in zymosan phagocytosis by macrophages. *J. Exp. Med.* 182:829–840.

Allen, L. A., and A. Aderem. 1996. Mechanisms of phagocytosis. *Curr. Opin. Immunol.* 8:36–40.

Bangham, A. D., M. W. Hill, and N. G. A. Miller. 1974. Preparation and use of liposomes: models of biological membranes. *Methods Membr. Biol.* 1:1–68.

Barlow, C. A., and J. R. MacDonald. 1967. Theory of discreteness of charge effects in the electrolyte compact double layer. *Adv. Electrochem. Electrochem. Eng.* 6:1–194.

Ben-Tal, N., B. Honig, C. Miller, and S. McLaughlin. 1997. Electrostatic binding of proteins to membranes: theoretical prediction and experimental results with charybdotoxin and phospholipid vesicles. *Biophys. J.* 73:1717–1727.

Ben-Tal, N., B. Honig, R. M. Peitzsch, G. Denisov, and S. McLaughlin. 1996. Binding of small basic peptides to membranes containing acidic lipids: theoretical models and experimental results. *Biophys. J.* 71: 561–575.

Bhatnagar, R. S., and J. I. Gordon. 1997. Understanding covalent modifications of proteins by lipids: where cell biology and biophysics mingle. *Trends Cell Biol.* 7:14–21.

Brooks, B. R., R. E. Bruccoleri, B. D. Olafson, D. J. States, S. Swaminathan, and M. Karplus. 1983. CHARMM: a program for macromolecular energy, minimization, and dynamics calculations. *J. Comp. Chem.* 4:187–217.

Buser, C. A., C. T. Sigal, M. D. Resh, and S. McLaughlin. 1994. Membrane binding of myristylated peptides corresponding to the NH_2-terminus of Src. *Biochemistry.* 33:13093–13101.

Cafiso, D., A. McLaughlin, S. McLaughlin, and A. Winiski. 1989. Measuring electrostatic potentials adjacent to membranes. *Methods Enzymol.* 171:342–364.

Chatelier, R. C., and A. P. Minton. 1996. Adsorption of globular proteins on locally planar surfaces: models for the effect of excluded area and aggregation of adsorbed protein on adsorption equilibria. *Biophys. J.* 71:2367–2374.

Dell'Acqua, M. L., M. C. Faux, J. Thorburn, A. Thorburn, and J. D. Scott. 1998. Membrane-targeting sequences on AKAP79 bind phosphatidyl-4,5-bisphosphate. *EMBO J.* 17:2246–2260.

Denisov, G., S. Wanaski, P. Luan, M. Glaser, and S. McLaughlin. 1997. Binding of basic peptides to membranes produces lateral domains enriched in the acidic lipids phosphatidylserine and phosphatidylinositol 4,5-bisphosphate: an electrostatic model and experimental results. *Biophys. J.* 74:731–744.

Epand, R. M., C. Stevenson, R. Bruins, V. Schram, and M. Glaser. 1998. The chirality of phosphatidylserine and the activation of protein kinase C. *Biochemistry.* 37:12068–12073.

Garnier, L., B. Bowzard, and J. W. Wills. 1998. Recent advances and remaining problems in HIV assembly. *AIDS.* 12:S5–S16.

Ghomashchi, F., X. Zhang, L. Liu, and M. H. Gelb. 1995. Binding of prenylated and polybasic peptides to membranes: affinities and intervesicle exchange. *Biochemistry.* 34:11910–11918.

Glaser, M., S. Wanaski, C. A. Buser, V. Boguslavsky, W. Rashidzada, A. Morris, M. Rebecchi, S. F. Scarlata, L. W. Runnels, G. D. Prestwich, J. Chen, A. Aderem, J. Ahn, and S. McLaughlin. 1996. MARCKS produces reversible inhibition of phospholipase C by sequestering phosphatidylinositol 4,5-bisphosphate in lateral domains. *J. Biol. Chem.* 271:26187–26193.

Grahame, D. C. 1958. Discreteness-of-charge-effects in the inner region of the electrical double layer. *Z. Elektrochem.* 62:264–274.

Hartsel, S. C., and D. S. Cafiso. 1986. A test of the discreteness-of-charge effects in phospholipid vesicles. *Biochemistry.* 25:8214–8219.

Heimburg, T., B. Angerstein, and D. Marsh. 1999. Binding of peripheral proteins to mixed lipid membranes: effect of lipid demixing upon binding. *Biophys. J.* 76:2575–2586.

Heimburg, T., and D. Marsh. 1995. Protein surface-distribution and protein-protein interactions in the binding of peripheral proteins to charged lipid membranes. *Biophys. J.* 68:536–546.

Holst, M. 1993. Numerical solutions to the finite-difference Poisson-Boltzmann equation. Ph.D. thesis, University of Illinois.

Holst, M., and F. Saied. 1993. Multigrid solution of the Poisson-Boltzmann equation. *J. Comp. Chem.* 14:105–113.

Honig, B. H., and A. Nicholls. 1995. Classical electrostatics in biology and chemistry. *Science.* 268:1144–1149.

Hope, M. J., M. B. Bally, G. Webb, and P. R. Cullis. 1985. Production of large unilamellar vesicles by a rapid extrusion procedure. Characterization of size distribution, trapped volume and ability to maintain a membrane potential. *Biochim. Biophys. Acta.* 812:55–65.

Hunter, R. J. 1981. Zeta Potential in Colloid Science. Academic Press, New York.

Kaplan, J. M., H. E. Varmus, and J. M. Bishop. 1990. The src protein contains multiple domains for specific attachment to membranes. *Mol. Cell. Biol.* 10:1000–1009.

Keller, S. L., W. H. Pitcher, III, W. H. Huestis, and H. M. McConnell. 1998. Red blood cell lipids form immiscible liquids. *Phys. Rev. Lett.* 81:5019–5022.

Kim, J., P. J. Blackshear, J. D. Johnson, and S. McLaughlin. 1994. Phosphorylation reverses the membrane association of peptides that correspond to the basic domains of MARCKS and neuromodulin. *Biophys. J.* 67:227–237.

Kim, J., M. Mosior, L. A. Chung, H. Wu, and S. McLaughlin. 1991. Binding of peptides with basic residues to membranes containing acidic phospholipids. *Biophys. J.* 60:135–148.

Kleinschmidt, J. H., and D. Marsh. 1997. Spin-label electron spin resonance studies on the interactions of lysine peptides with phospholipid membranes. *Biophys. J.* 73:2546–2555.

Knoblich, J. A., L. Y. Jan, and Y. N. Jan. 1997. The N terminus of the Drosophila Numb protein directs membrane association and actin-dependent asymmetric localization. *Proc. Natl. Acad. Sci. USA.* 94: 13005–13010.

Kwok, R., and E. Evans. 1981. Thermoelasticity of large lecithin bilayer vesicles. *Biophys. J.* 35:637–652.

Leventis, R., and J. R. Silvius. 1998. Lipid-binding characteristics of the polybasic carboxy-terminal sequence of K-ras4B. *Biochemistry.* 37: 7640–7648.

Levine, S., J. Mingins, and G. M. Bell. 1967. The discrete ion-effect in ionic double-layer theory. *J. Electroanal. Chem.* 13:280–329.

Liu, J., P. Oh, T. Horner, R. A. Rogers, and J. E. Schnitzer. 1997. Organized endothelial cell surface signal transduction in caveolae distinct from glycosylphosphatidylinositol-anchored protein microdomains. *J. Biol. Chem.* 272:7211–7222.

Liu, Y., L. Casey, and L. J. Pike. 1998. Compartmentalization of phosphatidlyinositol 4,5-bisphosphate in low-density membrane domains in the absence of caveolin. *Biochem. Biophys. Res. Commun.* 245: 684–690.

Maier, B., and J. O. Rädler. 1999. Conformation and self-diffusion of single DNA molecules confined to two dimensions. *Phys. Rev. Lett.* 82:1911–1914.

Martin, T. F. J. 1998. Phosphoinositide lipids as signaling molecules: common themes for signal transduction, cytoskeletal regulation, and membrane trafficking. *Annu. Rev. Cell Dev. Biol.* 14:231–264.

McConnell, H. M. 1991. Structures and transitions in lipid monolayers at the air-water interface. *Annu. Rev. Phys. Chem.* 42:171–195.

McIlroy, B. K., J. D. Walters, and J. D. Johnson. 1991. A continuous fluorescence assay for protein kinase C. *Anal. Biochem.* 195:148–152.

McLaughlin, S. 1989. The electrostatic properties of membranes. *Annu. Rev. Biophys. Biophys. Chem.* 18:113–136.

McLaughlin, S., and A. Aderem. 1995. The myristoyl-electrostatic switch: a modulator of reversible protein-membrane interactions. *Trends Biochem. Sci.* 20:272–276.

McLaughlin, S., N. Mulrine, T. Gresalfi, G. Vaio, and A. McLaughlin. 1981. Adsorption of divalent cations to bilayer membranes containing phosphatidylserine. *J. Gen. Physiol.* 77:445–473.

Möhwald, H. 1990. Phospholipid and phospholipid-protein monolayers and the air/water interface. *Annu. Rev. Phys. Chem.* 41:441–476.

Mosior, M., and S. McLaughlin. 1991. Peptides that mimic the pseudosubstrate region of protein kinase C bind to acidic lipids in membranes. *Biophys. J.* 60:149–159.

Mosior, M., and S. McLaughlin. 1992. Binding of basic peptides to acidic lipids in membranes: effects of inserting alanine(s) between the basic residues. *Biochemistry.* 31:1767–1773.

Mouritsen, O. G., and K. Jørgensen. 1997. Small-scale lipid-membrane structure: simulation versus experiment. *Curr. Opin. Struct. Biol.* 7:518–527.

Murray, D., N. Ben-Tal, B. Honig, and S. McLaughlin. 1997. Electrostatic interaction of myristoylated proteins with membranes: simple physics, complicated biology. *Structure.* 5:985–989.

Murray, D., L. Hermida-Matsumoto, C. A. Buser, J. Tsang, C. Sigal, N. Ben-Tal, B. Honig, M. D. Resh, and S. McLaughlin. 1998. Electrostatics and the membrane association of Src: theory and experiment. *Biochemistry.* 37:2145–2159.

Needham, D. 1993. Measurement of interbilayer adhesion energies. *Methods Enzymol.* 220:111–129.

Newton, A. C., and J. E. Johnson. 1998. Protein kinase C: a paradigm for regulation of protein function by two membrane-targeting modules. *Biochim. Biophys. Acta.* 1376:155–172.

Peitzsch, R. M., M. Eisenberg, K. A. Sharp, and S. McLaughlin. 1995. Calculations of the electrostatic potential adjacent to model phospholipid bilayers. *Biophys. J.* 68:729–738.

Pitcher, J. A., N. J. Freedman, and R. J. Lefkowitz. 1998. G protein-coupled receptor kinases. *Annu. Rev. Biochem.* 67:653–692.

Prendergast, F. G., M. Meyer, G. L. Carlson, S. Iida, and J. D. Potter. 1983. Synthesis, spectral properties, and use of 6-acryloyl-2-dimethylaminonaphthalene (acrylodan). *J. Biol. Chem.* 258:7541–7544.

Resh, M. D. 1996. Regulation of cellular signalling by fatty acid acylation and prenylation of signal transduction proteins. *Cell. Signal.* 8:403–412.

Rizo, J., and T. C. Sudhof. 1998. C2-domains, structure and function of a universal Ca^{2+}-binding domain. *J. Biol. Chem.* 273:15879–15882.

Roa, V. D., S. Misra, I. V. Boronenkov, R. A. Anderson, and J. H. Hurley. 1998. Structure of type IIβ phosphatidylinositol phosphate kinase: a protein kinase fold flattened for interfacial phosphorylation. *Cell.* 94: 829–839.

Rosen, A., K. F. Keenan, M. Thelen, A. C. Nairn, and A. Aderem. 1990. Activation of protein kinase C results in the displacement of its myristoylated, alanine-rich substrate from punctate structures in macrophage filopodia. *J. Exp. Med.* 172:1211–1215.

Seykora, J. T., M. M. Myat, L. A. Allen, J. V. Ravetch, and A. Aderem. 1996. Molecular determinants of the myristoyl-electrostatic switch of MARCKS. *J. Biol. Chem.* 271:18797–18802.

Sigal, C. T., W. Zhou, C. A. Buser, S. McLaughlin, and M. D. Resh. 1994. The amino terminal basic residues of Src mediate membrane binding through electrostatic interaction with acidic phospholipids. *Proc. Natl. Acad. Sci. USA.* 91:12253–12257.

Sutton, R. B., D. Fasshauer, R. Jahn, and A. T. Brunger. 1998. Crystal structure of a SNARE complex involved in synaptic exocytosis at 2.4 Å resolution. *Nature.* 395:347–353.

Swierczynski, S. L., and P. J. Blackshear. 1996. Myristoylation-dependent and electrostatic interactions exert independent effects on the membrane association of the myristoylated alanine-rich C-kinase substrate. *J. Biol. Chem.* 271:23424–23430.

Toner, M., G. Vaio, A. McLaughlin, and S. McLaughlin. 1988. Adsorption of cations to phosphatidylinositol 4,5-bisphosphate. *Biochemistry.* 27: 7435–7443.

Winiski, A. P., A. C. McLaughlin, R. V. McDaniel, M. Eisenberg, and S. McLaughlin. 1986. An experimental test of the discreteness-of-charge effect in positive and negative lipid bilayers. *Biochemistry.* 25: 8206–8214.

Yang, L., and M. Glaser. 1995. Membrane domains containing phosphatidylserine and substrate can be important for the activation of protein kinase C. *Biochemistry.* 34:1500–1506.

Yang, L., and M. Glaser. 1996. Formation of membrane domains during the activation of protein kinase C. *Biochemistry.* 35:13966–13974.

Zhou, W., L. J. Parent, J. W. Wills, and M. D. Resh. 1994. Identification of a membrane-binding domain within the amino-terminal region of human immunodeficiency virus type 1 Gag protein which interacts with acidic phospholipids. *J. Virol.* 68:2556–2569.